

# Quantification of Arterial and Venous Morphologic Markers in Pulmonary Arterial Hypertension Using CT Imaging



Farbod N. Rahaghi, MD, PhD; Pietro Nardelli, PhD; Eileen Harder, MD; Inderjit Singh, MD; Gonzalo Vegas Sánchez-Ferrero, PhD; James C. Ross, PhD; Rubén San José Estépar, MS; Samuel Y. Ash, MD; Andetta R. Hunsaker, MD; Bradley A. Maron, MD; Jane A. Leopold, MD; Aaron B. Waxman, MD, PhD; Raúl San José Estépar, PhD; and George R. Washko, MD



**BACKGROUND:** Pulmonary hypertension is a heterogeneous disease, and a significant portion of patients at risk for it have CT imaging available. Advanced automated processing techniques could be leveraged for early detection, screening, and development of quantitative phenotypes. Pruning and vascular tortuosity have been previously described in pulmonary arterial hypertension (PAH), but the extent of these phenomena in arterial vs venous pulmonary vasculature and in exercise pulmonary hypertension (ePH) have not been described. **RESEARCH QUESTION:** What are the arterial and venous manifestations of pruning and vascular tortuosity using CT imaging in PAH, and do they also occur in ePH?

**STUDY DESIGN AND METHODS:** A cohort of patients with PAH and ePH and control subjects with available CT angiograms were retrospectively identified to examine the differential arterial and venous presence of pruning and tortuosity in patients with precapillary pulmonary hypertension not confounded by lung or thromboembolic disease. The pulmonary vasculature was reconstructed, and an artificial intelligence method was used to separate arteries and veins and to compute arterial and venous vascular volumes and tortuosity.

**RESULTS:** A total of 42 patients with PAH, 12 patients with ePH, and 37 control subjects were identified. There was relatively lower (median [interquartile range]) arterial small vessel volume in subjects with PAH (PAH 14.7 [11.7-16.5;  $P < .0001$ ]) vs control subjects (16.9 [15.6-19.2]) and venous small vessel volume in subjects with PAH and ePH (PAH 8.0 [6.5-9.6;  $P < .0001$ ]; ePH, 7.8 [7.5-11.4;  $P = .004$ ]) vs control subjects (11.5 [10.6-12.2]). Higher large arterial volume, however, was only observed in the pulmonary arteries (PAH 17.1 [13.6-23.4;  $P < .0001$ ] vs control subjects 11.4 [8.1-15.4]). Similarly, tortuosity was higher in the pulmonary arteries in the PAH group (PAH 3.5 [3.3-3.6;  $P = .0002$ ] vs control 3.2 [3.2-3.3]).

**INTERPRETATION:** Lower small distal pulmonary vascular volume, higher proximal arterial volume, and higher arterial tortuosity were observed in PAH. These can be quantified by using automated techniques from clinically acquired CT scans of patients with ePH and resting PAH.

CHEST 2021; 160(6):2220-2231

**KEY WORDS:** arterial; CT imaging; exercise pulmonary hypertension; pulmonary arterial hypertension; tortuosity; venous

FOR EDITORIAL COMMENT, SEE PAGE 1998

**ABBREVIATIONS:** ePH = exercise pulmonary hypertension; PAH = pulmonary arterial hypertension

**AFFILIATIONS:** From Pulmonary and Critical Care Medicine (F. N. Rahaghi, E. Harder, S. Y. Ash, A. B. Waxman, and G. R. Washko), Department of Radiology (P. Nardelli, G. V. Sánchez-Ferrero, J. C. Ross, Rubén San José Estépar, A. R. Hunsaker, and Raúl San José Estépar), and the Division of Cardiovascular Medicine (B. A. Maron and J. A. Leopold), Brigham and Women's Hospital, Harvard Medical School, Boston, MA; and Pulmonary, Critical Care and Sleep (I. Singh), Yale School of Medicine, New Haven, CT. Drs Rahaghi and Nardelli are joint first authors.

Drs Raúl San José Estépar and Washko are joint senior authors.

**FUNDING/SUPPORT:** This study was supported in part by National Heart, Lung, and Blood Institute Grants [1K23HL136905, F. N. R.; 5R01HL116473, Raúl San José Estépar and G. R. W.; 1R01HL149877, Raúl San José Estépar; and 5K08HL145118, S. Y. A.].

**CORRESPONDENCE TO:** Farbod N. Rahaghi; email: [frahaghi@bwh.harvard.edu](mailto:frahaghi@bwh.harvard.edu)

Copyright © 2021 The Authors. Published by Elsevier Inc under license from the American College of Chest Physicians. This is an open access article under the CC BY-NC-ND license (<http://creativecommons.org/licenses/by-nc-nd/4.0/>).

**DOI:** <https://doi.org/10.1016/j.chest.2021.06.069>

## Take-home Points

**Study Question:** What are the arterial and venous manifestations of pruning and vascular tortuosity using CT imaging in PAH and ePH?

**Results:** Distal arterial and venous volume loss, proximal arterial dilation, and increased arterial tortuosity are observed on CT scans of patients with PAH and ePH.

**Interpretation:** Automated quantification methods using CT imaging can provide a noninvasive method for identification of PAH and ePH.

Pulmonary hypertension is a heterogeneous group of conditions that results from pathologic processes affecting the arteries, capillaries, or veins of the pulmonary vascular tree. Although right heart catheterization remains the gold standard for disease diagnosis and classification, this procedure is invasive, does not scale easily for screening large numbers of patients, and is used sparingly to monitor disease progression. For these reasons, noninvasive biomarkers are highly sought after for all aspects of clinical care. Cardiopulmonary imaging continues to show great promise as a noninvasive biomarker, and CT imaging in particular has become part of the standard clinical evaluation of patients with suspected pulmonary vascular disease. Numerous investigations have shown that CT imaging-based measures of the main pulmonary artery size, both alone and normalized by the diameter of the aorta,<sup>1</sup> are associated with the presence of pulmonary hypertension and are now commonly included in the clinical interpretation of a CT scan.<sup>2,3</sup> Less is known about the intraparenchymal vasculature and how the morphology of those arteries and veins may differ according to disease type.

A lower area of functional small vessel lumen is a histologic characteristic of pulmonary arterial

hypertension (PAH) that results in distal vascular pruning on pulmonary angiogram; this has been previously described by using taper and tree complexity measured by fractal dimension.<sup>4-6</sup> Studies have shown that pruning can be objectively assessed by using CT imaging and that its presence is clinically significant in COPD,<sup>7-9</sup> asthma,<sup>10</sup> and chronic thromboembolic disease.<sup>11</sup> In pulmonary hypertension, CT imaging-based sparsity of small vessels has also been characterized by using measures of tree complexity.<sup>12-14</sup> Increases in transmural pressure in the pulmonary vasculature due to elevated pulmonary vascular resistance may also lead to central vascular dilation,<sup>6,12,15</sup> much like the dilation of the main pulmonary artery or increased tortuosity.<sup>11,14</sup> However, the extent to which many of these morphologic changes differentially affect arteries and veins in patients with PAH has not yet been quantified in CT imaging. Characterization of the similarities and differences between arterial and venous changes in the lung parenchyma may enhance their utility as diagnostic markers and further improve the understanding of pulmonary vascular remodeling in PAH.

The goal of the current study was to quantify the changes in the parenchymal pulmonary arterial and venous vasculature in patients with PAH (Group 1 pulmonary hypertension) leveraging automated arterial and venous separation using an artificial intelligence algorithm. We hypothesized that lower small vessel volume, proximal vascular dilation, and higher vascular tortuosity would be found in the arteries but not veins of patients with PAH compared with control subjects. Secondarily, we sought to determine if those features detected in patients with PAH were also present in those with exercise pulmonary hypertension (ePH), which may be a pathophysiological precursor of PAH in some individuals.

## Subject and Methods

### Subject Selection

Subjects for this investigation were identified through a single-center registry consisting of 1,514 subjects who underwent right heart catheterization between April 27, 2011, and October 2, 2018. As shown in Figure 1, subjects were identified who had thin-slice CT angiography with fully visible lung fields and with the imaging occurring no more than 1 year following right heart catheterization. From this group, three cohorts of subjects (PAH, ePH, and control subjects) were identified.

Subjects with a resting mean pulmonary arterial pressure > 20 mm Hg and pulmonary vascular resistance > 3 Wood units were eligible for

inclusion in the PAH cohort (Fig 1). Exclusions criteria were an pulmonary arterial opening pressure > 15 mm Hg, CT evidence of thromboembolism, or clinical diagnosis of lung disease.<sup>16</sup> The remaining subjects diagnosed by pulmonary hypertension specialists as having Group 1 disease (PAH) without mixed disease (ie, presence of Group 2-5 disease) constituted the PAH cohort.

Subjects were eligible for inclusion in the ePH or control group if they had a resting mean pulmonary arterial pressure ≤ 20 mm Hg and had undergone invasive upright cardiopulmonary exercise testing to maximal exertion by a peak heart rate of > 85% predicted or a peak respiratory exchange ratio > 1.10. Subjects were excluded if they had lung disease either according to history or available spirometry,

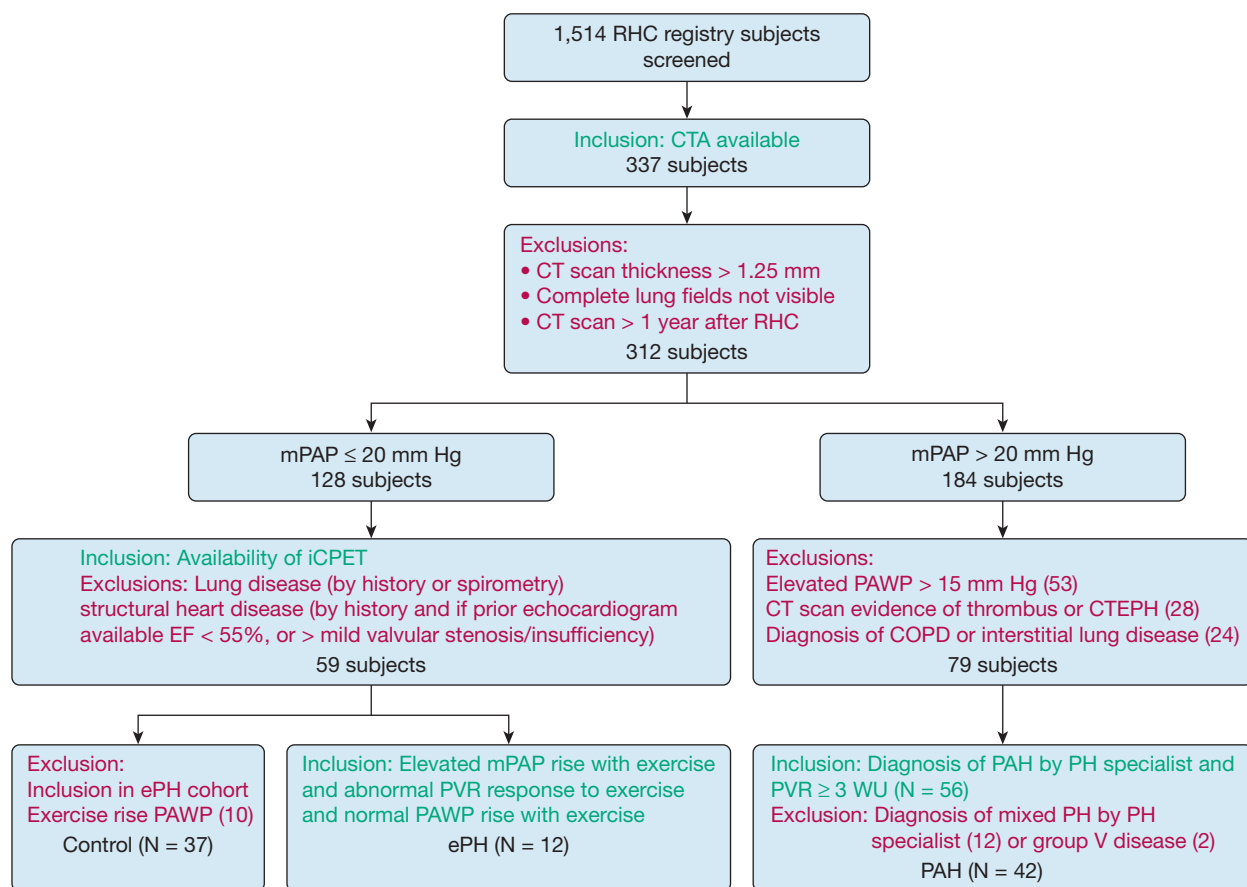


Figure 1 – Subject selection for the three groups of patients providing data for this study; the cohort is drawn from patients presenting for the work-up of unexplained dyspnea undergoing RHC. CTEPH = chronic thromboembolic pulmonary hypertension; CTPA = CT pulmonary angiogram; EF = ejection fraction; ePH = exercise pulmonary hypertension; iCPET = invasive cardiopulmonary exercise test; mPAP = mean pulmonary arterial pressure; PAH = pulmonary arterial hypertension; PAWP = pulmonary arterial wedge pressure; PH = pulmonary hypertension; PVR = pulmonary vascular resistance; RHC = right heart catheterization; WU = Wood unit.

structural heart disease by history or echocardiogram (or left ventricular ejection fraction < 50% or moderate/severe mitral or aortic valve disease), or significant shunting/hypoxemia with exercise.

Among the remaining group, subjects meeting the age-adjusted criteria of ePH<sup>17</sup> were selected. This included an elevated peak exercise mean pulmonary arterial pressure (> 30 mm Hg for age ≤ 50 years, > 33 mm Hg for age > 50 years), a blunted fall in pulmonary vascular resistance (> 1.34 Wood units at peak exercise ≤ 50 years old, > 2.10 for age > 50 years), and no evidence of age-adjusted elevated wedge pressures (pulmonary arterial wedge pressure > 19 mm Hg at peak exercise for age ≤ 50 years and > 17 mm Hg for age > 50 years). The remaining subjects with invasive upright cardiopulmonary exercise testing exhibiting no evidence of ePH or exercise-elevated wedge pressures were included as control subjects.

All subjects in this registry provided informed consent for a secondary analysis involving clinical data. This study was approved by the institutional review board (#2018P000419) at Mass General Brigham.

#### Methods of Automated Vascular Reconstruction and Quantification

A description of automated methods used for lung segmentation, vascular reconstruction, vascular labeling as arterial/venous, and

quantification of specific metrics are provided in e-Appendix 1. A visual summary of the process used is outlined in Figure 2. Briefly, the series with the thinnest axial sections were used to create a three-dimensional map of the lung parenchyma and perform vascular reconstruction using the Chest Imaging Platform ([www.chestimagingplatform.org](http://www.chestimagingplatform.org)),<sup>18,19</sup> which incorporates methods described in prior publications.<sup>7,20-23</sup> The vasculature was then labeled as arterial and venous by using a convolutional neural network.<sup>24</sup> The small, large, and total arterial and venous volumes were computed by using a previously used definition of 5 mm<sup>2</sup> as a cross-sectional area cutoff distinguishing large from small vessels.<sup>7,8,25,26</sup> Vascular volumes were normalized by the lung volume obtained from the same image. Distance from the chest wall was computed and expressed as a volumetric distance representing equal-volume concentric shells, with the center at the hilum, such that 0 would represent the chest wall and 1.0 would represent the hilum, and the volume distribution was plotted as a function of this distance for each individual. The method of computing tortuosity is summarized in the lower panel of Figure 2. Tortuosity was computed for each segment as previously described<sup>11</sup> and the median segment tortuosity reported for both the arterial and venous vessels. In addition, segments with tortuosity > 10% were counted in both the arterial and venous vessels, and the arterial count was normalized by the venous count (e-Appendix 1).

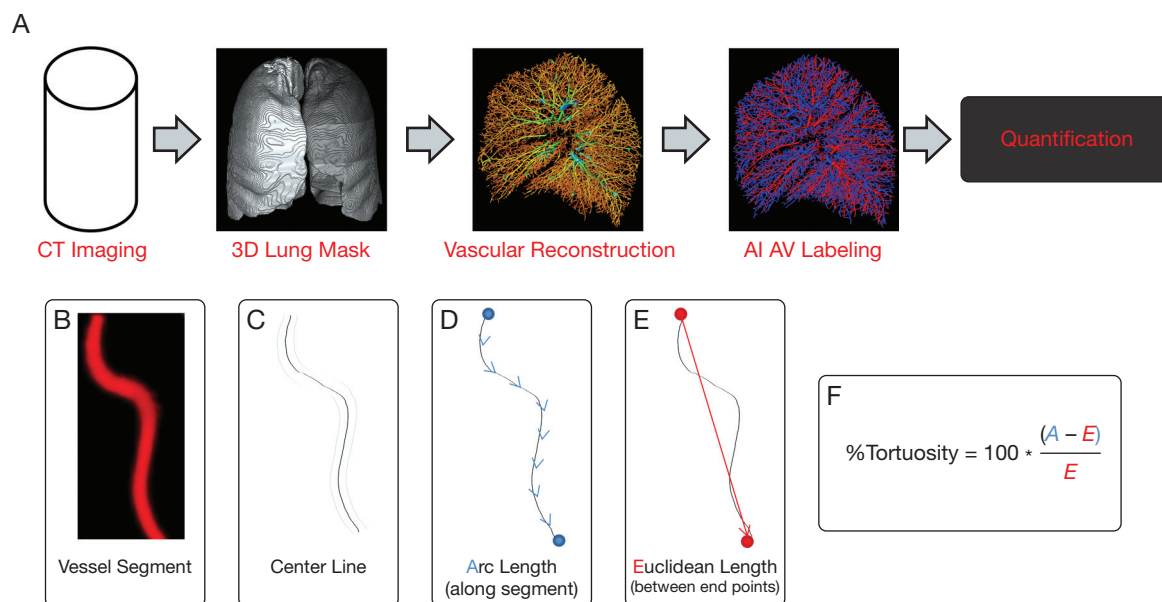


Figure 2 – A-F, A, Work-flow and process of getting from CT images to the quantification of vascular morphology used in this study is shown in panel A. The processes, including quantifications made, were all automated, although representative images were generated at each step to ensure that the results in each step were appropriate. Example of the measurement of percent tortuosity in an arterial vessel segment is shown in the bottom panels. B, In panel B, a selected vascular segment is shown in three-dimensional (3D) form. C, Panel C shows the centerline of the same vessel. D, The arc length is calculated by measuring the three-dimensional distance traversed by the vessel between its end points and labeled as arc length A (D). E, The Euclidean distance (straight line) is then measured between the end points and labeled E (E). F, The arc length is divided by the Euclidean end point distance and expressed as a percentage to yield the % tortuosity of the segment (F).

### Statistical Analysis

Data are presented as medians and interquartile ranges for continuous variables. Differences between groups were measured by using the

Mann-Whitney *U* test. Two sided *P* values are reported, and values < .05 were considered statistically significant. All statistical analysis was performed in R 4.0.1 (R Foundation for Statistical Computing).

## Results

The final study included 91 patients, with 42 subjects in the PAH group, 12 subjects in the ePH group, and 37 subjects in the control group. Demographic characteristics and resting hemodynamics for each group are presented in Table 1. The specific etiologies of PAH, the diagnosis associated with control subjects, and echocardiogram/pulmonary function test results are described in e-Appendix 2 (e-Table 1); the CT imaging parameters are described in e-Appendix 3 (e-Tables 2 and 3). For patients in the control and ePH groups, exercise capacity and hemodynamics from upright exercise testing are also provided in Table 1. The PAH and ePH groups were older than the control group, and the PAH and control groups included more female subjects than the ePH group.

Vascular reconstruction and quantification were performed by using the procedure as summarized in Figure 2. Examples of the three-dimensional reconstructions of the pulmonary vasculature and output from the artificial intelligence labeling of the

arterial and venous phase for a subject with PAH, a subject with ePH, and a control subject are shown in Figure 3. Additionally, graphs showing relative vascular volume as a function of vessel size for the same three subjects are shown in Figure 3, showing in these specific examples, lower distal vascular volume and proximal arterial dilation with disease.

CT imaging-based measures of lung and vascular volumes are presented in Table 2. The lung volumes and total vascular volumes (aggregate of arteries and veins, including small and large vessels) normalized by lung volume were similar between patients with PAH and control subjects. However, the small vessel volumes normalized by lung volume were lower in the PAH group compared with the control group, whereas the large vessel volumes normalized by lung volume were higher in the PAH group compared with the control group. The lung volumes and total vascular volumes were also similar between the ePH and control groups and similar to the PAH group; the ePH group had lower small vessel volumes

**TABLE 1 ] Demographic Characteristics, Hemodynamics, and Exercise Data of Subjects With PAH and ePH and Control Subjects**

Characteristic	PAH (n = 42)	ePH (n = 12)	Control (n = 37)
Age, y	64 (52-74)	65 (57-73)	53 (44-64)
Sex, female/male	35/7	3/9	28/9
Smoking history (> 5 pack-years)	19 (45)	3 (25)	13 (35)
Hypertension	21 (50)	3 (25)	15 (41)
Diabetes	6 (14)	1 (8.3)	5 (14)
Resting hemodynamics			
mPAP, mm Hg	42 (35-59)	18 (16-20)	18 (14-20)
PVR, WU	7.2 (5.6-9.8)	1.8 (1.4-2.3)	1.2 (1.0-1.7))
Resting supine cardiac output, L/min	4.7 (4.1-5.7)	5.4 (5.1-5.8)	5.1 (4.6-6.3)
Resting supine cardiac index, L/min/m <sup>2</sup>	2.6 (2.3-3.0)	2.7 (2.5-3.0)	2.9 (2.5-3.2)
PAWP, mm Hg	10 (7-12)	10 (7-10)	10 (8-13)
Days between RHC and CT scan	52 (7-244)	95 (31-250)	71 (8-159)
Exercise hemodynamics <sup>a</sup>			
VO <sub>2max</sub> % predicted	...	61 (59-71)	81 (68-92)
Peak exercise mPAP, mm Hg	...	39 (35-43)	20 (17-30)
Peak exercise PAWP, mm Hg	...	16 (14-17)	10 (5-13)
Peak exercise PVR, WU	...	2.3 (2.0-3.5)	1.3 (0.9-1.6)
Peak mPAP/cardiac output (TPR), mm Hg • min/L	...	3.7 (3.4-5.9)	2.0 (1.6-2.4)

Data are presented as median (interquartile range) or No. (%), except for sex, which is expressed as a ratio. ePH = exercise pulmonary hypertension; mPAP = mean pulmonary arterial pressure; PAH = pulmonary arterial hypertension; PAWP = pulmonary arterial wedge pressure; PVR = pulmonary vascular resistance; RHC = right heart catheterization; VO<sub>2max</sub> = maximum oxygen consumption WU = Wood units.

<sup>a</sup>All control subjects and subjects with ePH by definition had undergone invasive exercise testing. Most patients with resting evidence of PAH did not undergo invasive exercise testing.

compared with control subjects, but the trend of higher large vessel volume did not reach statistical significance.

Analyses of the arterial and venous vasculature by vessel size are summarized in [Table 2](#) with validation of arterial and venous separations using manual labeling as described in [e-Appendix 4 \(e-Tables 4 and 5\)](#). The lung volume-normalized total arterial volume was greater in the PAH cohort compared with the control cohort. This finding reflected a lower lung volume-normalized small arterial vessel volume and higher lung volume-normalized arterial large vessel volume compared with control subjects. Although there was a trend for the higher total and large vessel and lower small vessel arterial volume when comparing subjects with ePH vs control subjects, these findings did not reach statistical significance.

A similar analysis of the venous vasculature revealed a lower lung volume-normalized total venous volume in subjects with PAH compared with control subjects, resulting from a lower lung volume-normalized venous small vessel volume. The lung normalized-venous large vessel volumes were similar between the PAH and control groups. As in the PAH group, there was also lower lung

volume-normalized venous small vessel volume in the ePH group compared with the control group. The venous total and large vessel volumes did not exhibit a difference between subjects with ePH and control subjects. The key findings from the arterial and venous volume vessel size-based analysis are summarized in [Figure 4](#).

Normalization of the arterial vascular volume by venous vascular volume is described in [Table 2](#). The ratio of arterial to venous vascular volume (AV ratio) was higher in subjects with PAH compared with control subjects, which reflected a higher AV ratio both for small vessels and large vessels. When comparing the ePH group vs the control group, there was similarly a higher total AV ratio, although only the difference in large vessel AV ratio reached statistical significance.

Acknowledging that “small” and “large” vessel designations is an imprecise representation of distal and proximal locations in the vascular tree, the arterial and venous vasculature was then stratified based on volumetric distance from the chest wall, as shown in [Figure 5](#). Vascular volume was plotted as a function of the volumetric distance from the chest wall for all



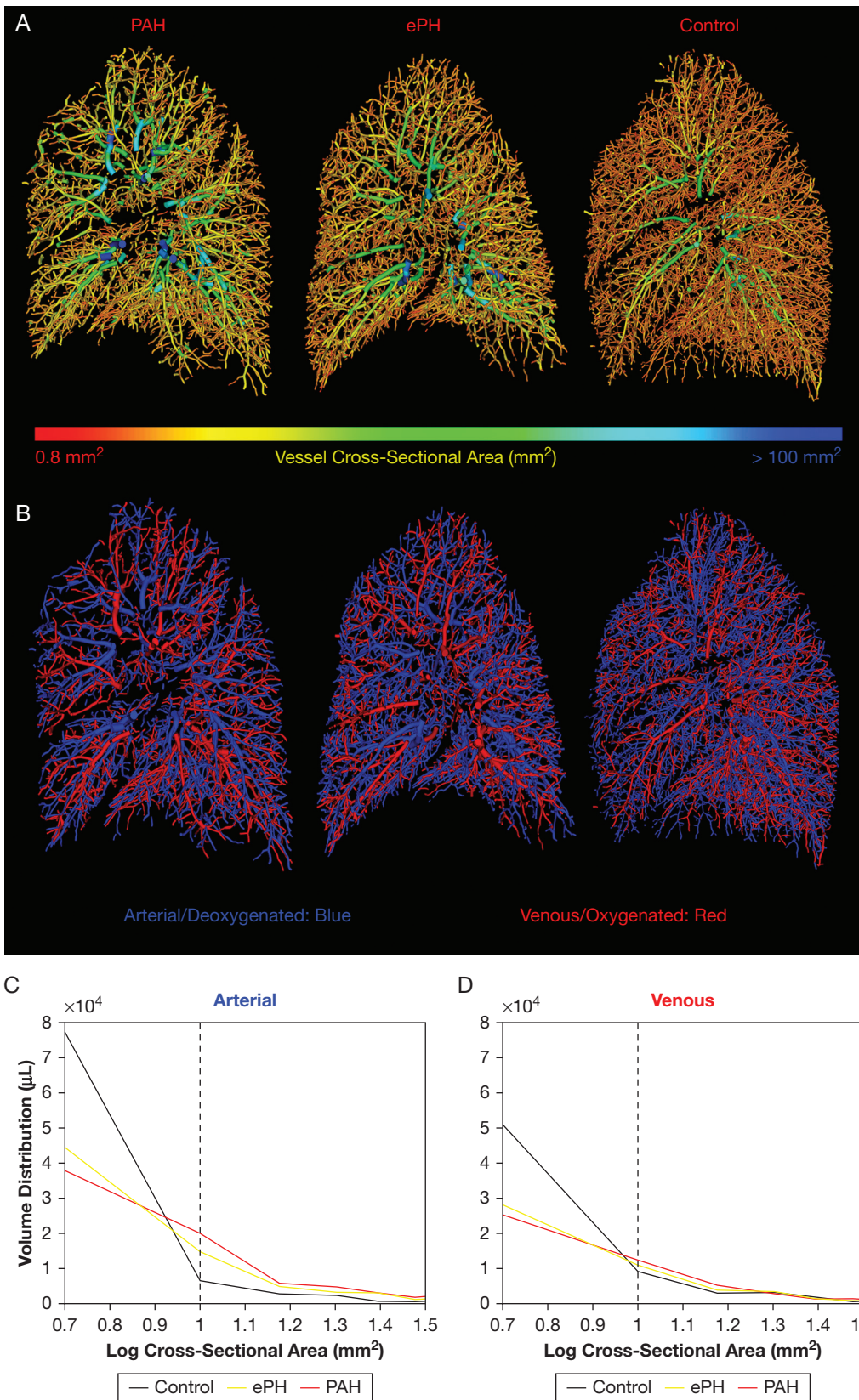


Figure 3 – A, Examples of vascular reconstructions for three subjects, one with resting PAH (left), one with ePH (middle), and a control subject (right). The coloring represents the cross-sectional area of the vessel, with blue vessels being the largest. Note the higher volume encompassed by proximal large vessel volume (blue) and lower volume and count of distal small vessels (red) in the subject with PAH compared with the control subject. (Continued)

**TABLE 2 ] CT Imaging-Derived Quantification of Vascular Volume (Normalized by Lung Volume) Distribution Based on Vessel Cross-Sectional Area**

Measurement	PAH (n = 42)	ePH (n = 12)	Control Subject (n = 37)	PAH vs Control Subject <sup>a</sup>	ePH vs Control Subject <sup>a</sup>
Lung volume, L	3.1 (2.7-3.9)	3.4 (2.7-4.2)	3.7 (2.7-4.4)	.22	.65
Total vessel volume <sup>b</sup>	49.4 (44.9-57.9)	52.2 (47.1-56.3)	48.4 (43.6-54.3)	.59	.38
Small vessel volume	23.4 (18.5-25.9)	22.5(18.7-29.5)	28.9 (25.9-31.4)	< .0001	.03
Large vessel volume	26.6 (21.7-36.4)	24.3 (19.4-36.9)	21.4 (14.8-25.2)	.0004	.11
<b>Arterial vascular measures</b>					
Total arterial volume	33.2 (28.8-37.8)	32.6 (30.0-35.1)	28.9 (25.5-34.1)	.02	.15
Small arterial volume	14.7 (11.7-16.5)	14.8 (12.0-18.3)	16.9 (15.6-19.2)	< .0001	.08
Large arterial volume	17.1 (13.6-23.4)	14.7 (11.9-22.7)	11.4 (8.1-15.4)	< .0001	.06
<b>Venous vascular measures</b>					
Total venous volume	17.4 (14.9-19.7)	18.6 (16.9-20.7)	19.6 (18.3-21.1)	.0007	.33
Small venous volume	8.0 (6.5-9.6)	7.8 (7.5-11.4)	11.5 (10.6-12.2)	< .0001	.004
Large venous volume	8.0 (7.4-10.2)	9.1 (7.2-10.9)	8.3 (7.3-9.6)	.87	.53
<b>Arterial adjusted by venous</b>					
Total AV ratio	1.82 (1.60-2.36)	1.67(1.60-1.78)	1.47 (1.32-1.70)	< .0001	.02
Small vessel AV ratio	1.74 (1.61-1.93)	1.65 (1.59-1.81)	1.57 (1.40-1.68)	< .0001	.05
Large vessel AV ratio	1.94 (1.68-2.79)	1.64 (1.60-1.70)	1.31 (1.13-1.70)	< .0001	.02

Data are presented as median (interquartile range). AV ratio = the ratio of arterial to venous volume; ePH = exercise pulmonary hypertension; PAH = pulmonary arterial hypertension.

<sup>a</sup>P values represent two-sided significance from the Mann-Whitney U test.

<sup>b</sup>All vascular volumes are normalized by lung volumes. The resulting measure when normalizing by lung volume is a unit-less value representing milliliters of vessel per liters of lung.

patients, and the peak in vascular volume identified as described in e-Appendix 1 and summarized in Table 3. The peak in vascular volume in PAH was shifted toward the hilum in both the arterial and venous trees. The same shift toward the hilum was noted when comparing subjects with ePH vs control subjects.

Lastly, vascular tortuosity was computed as described in Figure 2 for both arteries and veins (Table 4). The median tortuosity was higher in patients with PAH (but not ePH) compared with the control group, whereas the

median tortuosity for the venous vasculature was the same. Examples of the arterial tree with tortuous vessel segments based on different thresholds for three subjects, as well as a histogram of vessel tortuosity, are shown in Figure 6. Motivated in part by the relatively higher number of tortuous segments in the tail of this distribution, we calculated the ratio of the number of tortuous arterial segments (ie, segments with > 10% tortuosity) to the number of tortuous venous segments (AV ratio segments > 10.0% tortuosity as shown in Table 4), which was higher in subjects with

**Figure 3 | (Continued) B, Arterial/venous-labeled versions of the same reconstructions are presented. These are used to quantify the vascular volume as a function of vessel size. In the lower panels, relative vascular volume distribution is shown as a function of cross-sectional area for the arterial (C) and venous (D) circulation. Note the lower small vessel volume both on the arterial and venous side in the subjects with PAH and ePH and the higher proximal arterial vessel volume in the arterial side close to a cross-sectional area of 10 mm<sup>2</sup> (location of the vertical dotted line). ePH = exercise pulmonary hypertension; PAH = pulmonary arterial hypertension.**

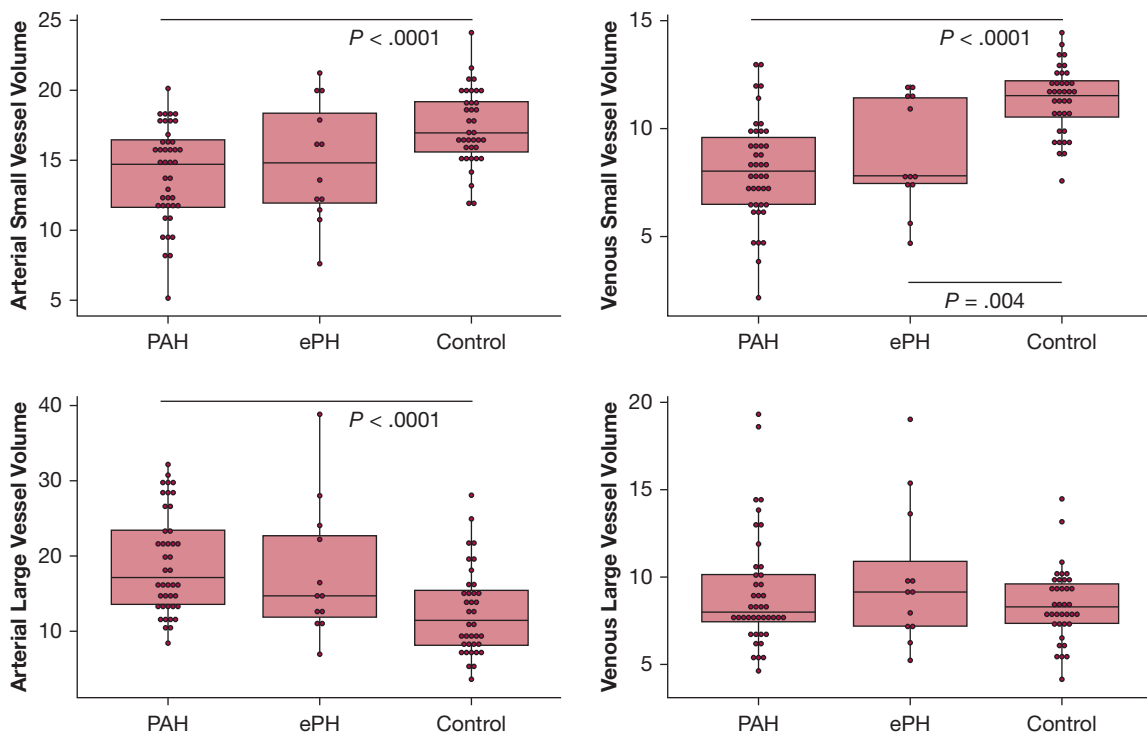


Figure 4 – Small and large vessel volume distributions for the arterial and venous pulmonary vascular trees (values and comparisons shown in Table 2). The arterial and venous small vessel volumes (top panels) show lower volumes in subjects with PAH compared with control subjects, with the ePH subjects having a statistically significant difference for the venous tree. For the large vessel volume, higher volumes were obtained in subjects with PAH compared with control subjects only in the arterial tree (bottom panels). ePH = exercise pulmonary hypertension; PAH = pulmonary arterial hypertension.

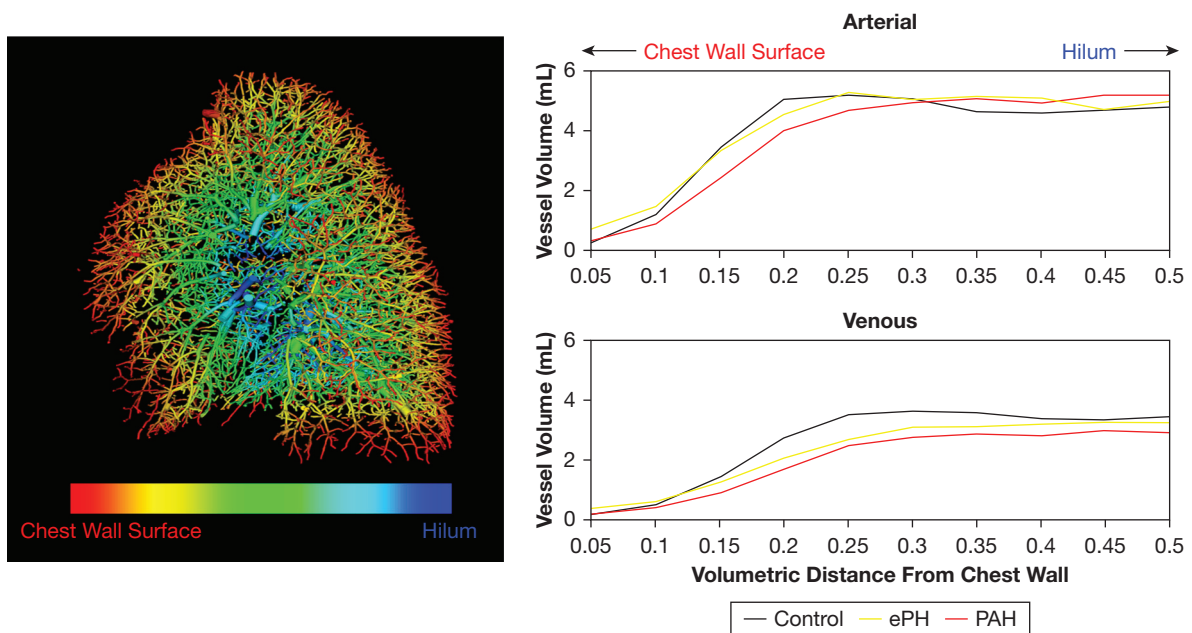


Figure 5 – The vasculature labeled as a function of distance from the surface of the chest wall (left) with red indicating close to the chest wall and blue indicating vessels close to the mediastinum. The panel on the right shows the vascular volume density as a function of normalized distance to the chest wall, with control subjects (black), subjects with ePH (yellow), and those with resting PAH (red) shown for both arterial (top) and venous (bottom) vessels. In both arterial and venous vasculature, there is a peak in vascular volume between one-fifth (0.2) to one-half (0.5) of the way from the chest wall to hilum. For both ePH and PAH, the peak is shifted closer to the hilum. In the arterial system, although the subjects with PAH start with lower distal volumes, there is a more sharp increase of volume toward the proximal direction as the increased arterial dilation contributes more volume proximally. On the venous side, the peak vascular volume density is lower and less prominent in the venous circulation for patients with ePH and PAH compared with control subjects. ePH = exercise pulmonary hypertension; PAH = pulmonary arterial hypertension.



**TABLE 3 ] CT Imaging-Derived Quantification of Vascular Volume Based on Spatial Distribution**

Measurement	PAH (n = 42)	ePH (n = 12)	Control Subject (n = 37)	PAH vs Control Subject <sup>a</sup>	ePH vs Control Subject <sup>a</sup>
Arterial peak location	0.35 (0.25-0.43)	0.40 (0.25-0.46)	0.25 (0.20-0.30)	.0003	.01
Venous peak location	0.45 (0.35-0.50)	0.45 (0.39-0.46)	0.30 (0.25-0.35)	< .00001	.001

Data are presented as median (interquartile range). ePH = exercise pulmonary hypertension; PAH = pulmonary arterial hypertension.

<sup>a</sup>P values represent two-sided significance from Mann-Whitney *U* test.

PAH and ePH compared with control subjects. Logistic regression-based analysis of key variables with adjustments for sex and age are presented in [e-Appendix 5 \(e-Table 6\)](#).

## Discussion

In this single-center retrospective examination of our right heart catheterization research registry, we identified a group of patients with PAH, a group with ePH, and patients without any evidence of pulmonary vascular disease detected by invasive upright cardiopulmonary exercise testing designated as control subjects. Using CT images, volumetric reconstructions of the intraparenchymal pulmonary arterial and pulmonary venous vascular trees were generated, and several metrics from those trees were extracted to objectively compare their morphology. Measures of discrete vascular volumes as well as volume measures plotted as a function of distance from the chest wall exhibited distal arterial and venous pruning in patients with PAH and ePH; proximal arterial dilation was limited to those with PAH. We further examined vascular tortuosity and found those metrics in the arterial but not venous

vasculature to be higher in subjects with PAH compared with control subjects.

Pruning, or sparsity of the small or distal vasculature, has been previously described in patients with pulmonary vascular disease. We used two different approaches to assess this process in the arterial and venous vascular trees. The measures of blood vessel volume < 5 mm<sup>2</sup> in cross-section have been described in detail in several previous publications,<sup>7,9,23</sup> but the technique using the distribution of vessel volume as a function of volumetric distance from the chest wall is unique to this investigation. We introduced this latter approach to better illustrate the shift in vessel volume to the central vasculature in disease but also because discrete measures of small vessel volume may underestimate the impact of disease on vascular morphology. For example, as pruning of the vascular tree progresses, larger distal vessels may shrink in size, and if their cross-sectional area drops below 5 mm<sup>2</sup>, their addition to the small vessel volume metric will effectively increase volume measures in this range. This additive effect is counterbalanced by the lack of small vessels when they fall below the limits of resolution of clinical CT scanning and no longer contribute volume

**TABLE 4 ] CT Imaging-Derived Quantification of Arterial and Venous Tortuosity**

Measurement	PAH (n = 42)	ePH (n = 12)	Control Subject (n = 37)	PAH vs Control Subject <sup>a</sup>	ePH vs Control Subject <sup>a</sup>
<b>Arterial</b>					
Median arterial tortuosity (%) <sup>b</sup>	3.5 (3.3-3.6)	3.3 (3.1-3.4)	3.2 (3.2-3.3)	.0002	.95
<b>Venous</b>					
Median venous tortuosity (%)	2.9 (2.7-3.0)	2.7 (2.6-2.9)	2.8 (2.7-3.0)	.12	.28
<b>Arterial adjusted by venous</b>					
AV ratio segments > 10.0% tortuosity	2.0 (1.6-2.8)	1.9 (1.7-2.0)	1.5 (1.3-1.7)	< .0001	.02

Data are presented as median (interquartile range). ePH = exercise pulmonary hypertension; PAH = pulmonary arterial hypertension.

<sup>a</sup>P values represent two-sided significance from the Mann-Whitney *U* test.

<sup>b</sup>Percent tortuosity is the additional length of the segment above what would be a straight line connecting the end points, such that a straight segment would have a tortuosity of 0%.

measures in this range. It is only when vascular loss exceeds the addition of “shrinking” vessels that the volume encompassed by small vessels will decrease.

We measured distal pruning by identifying the peak vascular volume as a function of distance from the chest wall: in a pruned vascular tree, this peak appears closer to the mediastinum as the distal vessels lose volume and the more proximal vessels dilate due to increased resistance to flow. We observed pruning of the distal arterial and venous vascular trees in patients with PAH. More surprising, however, was this same observation of vascular pruning in patients with ePH. Pruning of the distal arterial vasculature is a well-documented pathological process in PAH, and targeting the lower cross-sectional area of precapillary blood vessels through vasodilation or reversal of vascular remodeling forms the foundation of clinical care for these patients. The presence of distal arterial pruning in patients with ePH corroborates growing evidence that ePH may represent an early form of PAH. Intraparenchymal proximal arterial dilation is likely related to the dilation of the main pulmonary artery also observed in this cohort (e-Table 7, e-Appendix 6). The presence of proximal arterial dilation (higher vascular volumes) in PAH but not ePH suggests that the increase in pulmonary vascular resistance and lower arterial compliance associated with pruning evident on CT scan in the latter subgroup is not great enough at rest to result in elevations of transmural pressure and proximal vascular enlargement. It is possible that repetition of the same CT studies during exercise would show more proximal dilation of the arterial vasculature in proportion to increases in pulmonary arterial pressure during exertion. Pruning of the distal venous vasculature in patients with both PAH and ePH on CT imaging is likely related to a reduced local perfusion, although we cannot rule out a concurrent process such as venous remodeling seen in pulmonary venoocclusive disease. A detailed spatial matching of the arterial and venous vascular trees may provide insight into whether the loss of distal venous volume is spatially matched to the local changes in the arteries.

Previous subjective and objective CT imaging-based investigations have reported higher tortuosity of the intraparenchymal pulmonary vasculature in patients with PAH.<sup>14</sup> We subsequently found in patients with chronic thromboembolic pulmonary hypertension that this process was limited to the arterial vascular tree,<sup>11</sup> but such an examination has not been reported in patients with Group 1 PAH. In the current investigation,

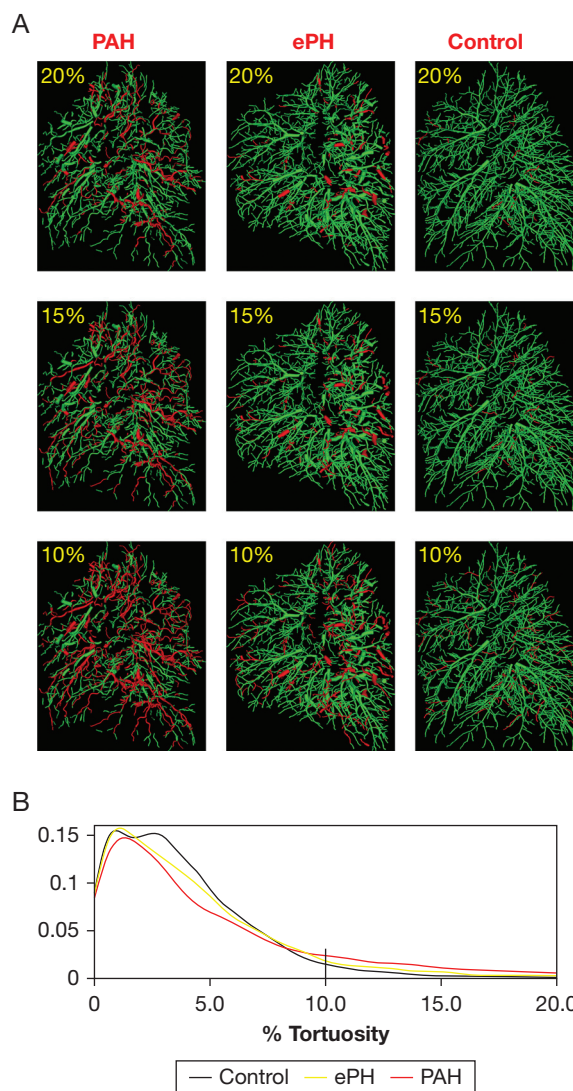


Figure 6 – A, Examples of tortuous vessels in three subjects with resting PAH (left panels), ePH (middle panels), and a control subject (right panels). Vessels are marked as red if exceeding a tortuosity of 20% (top), 15% (middle), or 10% (bottom). B, Estimated probability distribution derived from the data for each subject, in which the larger relative number of high tortuosity segments (> 10% tortuosity, delineated by the black vertical line) is shown in the patient with PAH compared with the control subject. An increase in the number of tortuous vessel segments is seen around 8% to 10%, which motivated the selection of 10% as a cutoff for “high tortuosity.” ePH = exercise pulmonary hypertension; PAH = pulmonary arterial hypertension.

vessel segment tortuosity was measured in the arterial and then venous pulmonary circulation, and we found that, similar to chronic thromboembolic pulmonary hypertension, patients with Group 1 PAH have higher median arterial but not venous vascular tortuosity. Our preliminary work exploring the ratio of tortuous arterial to venous vascular segments suggests that patients with ePH may have subtle higher arterial vascular tortuosity compared with control subjects.

There are several limitations of this investigation that must be acknowledged. This was a retrospective study, and the analysis was limited to the subset of patients who had CT images available for processing. The limitation of the available sample is particularly germane for the analysis of subjects with ePH, who had a markedly different sex composition than the control and PAH groups and a higher median time between CT imaging and right heart catheterization. This availability will also reflect a clinical bias; that is, the subjects who had scans were those in whom a clinician felt the scan was warranted for clinical care, which may affect the generalizability of our findings. In addition, the small sample size and limited a priori knowledge of effect size estimates make it possible that the study was underpowered to detect some of the differences between cohorts. Although the current control cohort had no evidence of pulmonary vascular disease following extensive testing, they were referred for symptomatic dyspnea and cannot be considered as completely “healthy” control subjects. CT scans were used if they were acquired within 1 year following the date of right heart catheterization, during which therapy for PAH may have been initiated. The impact of therapy on vascular morphology is unknown, but it is possible that with improvement in hemodynamics, there would be an underestimation of the differences between control subjects and subjects with PAH. It is possible that disease leads to changes in the quality of imaging (eg,

ability to hold full breath, additional motion artifact) that could affect the results of this analysis. In addition, interstitial lung disease and restrictive lung disease often complicate PAH, particularly in the context of connective tissue disease. A sensitivity analysis addressing this topic is presented in [e-Appendix 7 \(e-Table 8\)](#). CT scans were obtained in the supine position, which is different from the testing conditions used to diagnose ePH. Finally, this article examined many different derived quantities, and the number of comparisons increases the probability of chance statistical significance. Prospective validation is necessary to confirm these findings and assess their utility in specific clinical contexts.

### Interpretation

Distal pruning and proximal dilation as well as higher tortuosity of the arterial vasculature are all evident on the CT scans of patients with PAH. Vascular pruning is also evident in patients with ePH, suggesting that in at least some subjects, this may represent an early form of PAH. This finding suggests that objective CT imaging-based assessments of the pulmonary vasculature may be used to detect certain forms of pulmonary vascular disease. Further work is needed to determine the sensitivity and specificity of such metrics as well as their value for prognostication and monitoring response to therapeutic intervention.

## Acknowledgments

**Author contributions:** F. N. R. is the guarantor of the paper, taking responsibility for the integrity of the work as a whole, from inception to published article. F. N. R., P. N., A. B. W., Raúl San José Estépar, B. M., J. A. L., I. S., A. R. H., and G. R. W. were involved in the conceptualization; and F. N. R., P. N., E. H., I. S., G. V. S. F., J. C. R., Raúl San José Estépar, S. Y. A., Rubén San José Estépar, and A. R. H. were involved in data collection and analysis. All authors participated in writing and approval of the final manuscript.

**Financial/nonfinancial disclosures:** The authors have reported to *CHEST* the following: Raúl San José Estépar. reports grants from the National Institutes of Health, National Heart, Lung, and Blood Institute, during the conduct of the study; personal fees from Leuko Labs; grants and personal fees from Boehringer Ingelheim; and personal fees from Chiesi USA Inc. G. R. W. reports grants from the National Institutes of Health; grants and other from Boehringer Ingelheim and Janssen Pharmaceuticals; other from Quantitative Imaging Solutions and PulmonX; other from GlaxoSmithKline, Novartis, Vertex, and CSL Behring, outside the submitted work; and his spouse works for Biogen. Raúl San José Estépar and G. R. W. are also founders and co-owners of Quantitative Imaging Solutions, which is a company that provides image-based consulting and develops software to enable data-sharing. None declared (F. N. R., P. D., E. H., I. S., G. V. S.-F., J. C. R., R. S. J. E., S. Y. A., A. R. H., B. A. M., J. A. L., A. B. W.).

**Role of sponsors:** The sponsor had no role in the design of the study, the collection and analysis of the data, or the preparation of the manuscript.

**Additional information:** The e-Appendixes and e-Tables can be found in the Supplemental Materials section of the online article.

## References

1. Ng CS, Wells AU, Padley SP. A CT sign of chronic pulmonary arterial hypertension: the ratio of main pulmonary artery to aortic diameter. *J Thorac Imaging*. 1999;14(4):270-278.
2. Johns CS, Wild JM, Rajaram S, Swift AJ, Kiely DG. Current and emerging imaging techniques in the diagnosis and assessment of pulmonary hypertension. *Expert Rev Respir Med*. 2018;12(2):145-160.
3. Devaraj A, Wells AU, Meister MG, Corte TJ, Wort SJ, Hansell DM. Detection of pulmonary hypertension with multidetector CT and echocardiography

- alone and in combination. *Radiology*. 2010;254(2):609-616.
4. Reid L. The angiogram and pulmonary artery structure and branching (in the normal and with reference to disease). *Proc R Soc Med*. 1965;58(9):681-684.
5. Rabinovitch M, Keane JF, Fellows KE, Castaneda AR, Reid L. Quantitative analysis of the pulmonary wedge angiogram in congenital heart defects. Correlation with hemodynamic data and morphometric findings in lung biopsy tissue. *Circulation*. 1981;63(1):152-164.
6. Boxt LM, Katz J, Liebovitch LS, Jones R, Esser PD, Reid L. Fractal analysis of pulmonary arteries: the fractal dimension is lower in pulmonary hypertension. *J Thorac Imaging*. 1994;9(1):8-13.
7. Estépar RS, Kinney GL, Black-Shinn JL, et al; COPDGene Study. Computed tomographic measures of pulmonary vascular morphology in smokers and their clinical implications. *Am J Respir Crit Care Med*. 2013;188(2):231-239.
8. Matsuoka S, Washko GR, Yamashiro T, et al. Pulmonary hypertension and computed tomography measurement of small pulmonary vessels in severe emphysema. *Am J Respir Crit Care Med*. 2010;181(3):218-225.
9. Rahaghi FN, Argemi G, Nardelli P, et al. Pulmonary vascular density: comparison of findings on computed tomography imaging with histology. *Eur Respir J*. 2019;54(2).
10. Ash SY, Rahaghi FN, Come CE, et al; SARP Investigators. Pruning of the pulmonary vasculature in asthma. The Severe Asthma Research Program (SARP) Cohort. *Am J Respir Crit Care Med*. 2018;198(1):39-50.
11. Rahaghi FN, Ross JC, Agarwal M, et al. Pulmonary vascular morphology as an imaging biomarker in chronic thromboembolic pulmonary hypertension. *Pulm Circ*. 2016;6(1):70-81.
12. Moledina S, de Bruyn A, Schievano S, et al. Fractal branching quantifies vascular changes and predicts survival in pulmonary hypertension: a proof of principle study. *Heart*. 2011;97(15):1245-1249.
13. Haitao S, Ning L, Lijun G, Fei G, Cheng L. Fractal dimension analysis of MDCT images for quantifying the morphological changes of the pulmonary artery tree in patients with pulmonary hypertension. *Korean J Radiol*. 2011;12(3):289-296.
14. Helmberger M, Pienn M, Urschler M, et al. Quantification of tortuosity and fractal dimension of the lung vessels in pulmonary hypertension patients. *PLoS One*. 2014;9(1):e87515.
15. Reid LM. Structure and function in pulmonary hypertension. New perceptions. *Chest*. 1986;89(2):279-288.
16. Simonneau G, Montani D, Celermajer DS, et al. Haemodynamic definitions and updated clinical classification of pulmonary hypertension. *Eur Respir J*. 2019;53(1):1801913.
17. Oliveira RK, Agarwal M, Tracy JA, et al. Age-related upper limits of normal for maximum upright exercise pulmonary haemodynamics. *Eur Respir J*. 2016;47(4):1179-1188.
18. San Jose Estepar R, Ross JC, Harmouche R, Onieva J, Diaz AA, Washko GR. Chest imaging platform: an open-source library and workstation for quantitative chest imaging. *C66 Lung Imaging II: New Probes and Emerging Technologies*. American Thoracic Society; 2015:A4975.
19. Onieva JRJ, Harmouche R, Yarmarkovich A, et al. Chest Imaging Platform: an open-source library and workstation for quantitative chest imaging. *Int J Comput Assist Radiol Surg*. 2016;11(suppl 1):S40-S41.
20. Ross JC, Estepar RS, Diaz A, et al. Lung extraction, lobe segmentation and hierarchical region assessment for quantitative analysis on high resolution computed tomography images. *Med Image Comput Comput Assist*. 2009;12(pt 2):690-698.
21. Ross JC, Kindlmann GL, Okajima Y, et al. Pulmonary lobe segmentation based on ridge surface sampling and shape model fitting. *Medical Physics*. 2013;40(12):121903.
22. Kindlmann GL, San Jose Estepar R, Smith SM, Westin CF. Sampling and visualizing creases with scale-space particles. *IEEE Trans Vis Comput Graph*. 2009;15(6):1415-1424.
23. Estépar RS, Ross JC, Krissian K, Schultz T, Washko GR, Kindlmann GL. Computational vascular morphometry for the assessment of pulmonary vascular disease based on scale-space particles. *Proc IEEE Int Symp Biomed Imaging*. 2012:1479-1482.
24. Nardelli P, Jimenez-Carretero D, Bermejo-Pelaez D, et al. Pulmonary artery-vein classification in CT images using deep learning. *IEEE Trans Med Imaging*. 2018;37(11):2428-2440.
25. Washko GR, Nardelli P, Ash SY, et al. Arterial vascular pruning, right ventricular size, and clinical outcomes in chronic obstructive pulmonary disease. A longitudinal observational study. *Am J Respir Crit Care Med*. 2019;200(4):454-461.
26. Washko GR, Nardelli P, Ash SY, et al. Smaller left ventricle size at noncontrast CT is associated with lower mortality in COPDGene Participants. *Radiology*. 2020;296(1):208-215.